Title
Spatiotemporal encoding of search strategies by prefrontal neurons

Journal
Proceedings of the National Academy of Sciences of the United States of America, 115(19)

ISSN
0027-8424

Authors
Chiang, Feng-Kuei
Wallis, Joni D

Publication Date
2018-05-08

DOI
10.1073/pnas.1805044115

Peer reviewed

Spatiotemporal encoding of search strategies by prefrontal neurons

Feng-Kuei Chiang[a,1] and Joni D. Wallis[a,b,2]

[a]Department of Psychology, University of California, Berkeley, CA 94720; and [b]Helen Wills Neuroscience Institute, University of California, Berkeley, CA 94720

Edited by Robert Desimone, Massachusetts Institute of Technology, Cambridge, MA, and approved April 4, 2018 (received for review March 27, 2018)

Working memory is capacity-limited. In everyday life we rarely notice this limitation, in part because we develop behavioral strategies that help mitigate the capacity limitation. How behavioral strategies are mediated at the neural level is unclear, but a likely locus is lateral prefrontal cortex (LPFC). Neurons in LPFC play a prominent role in working memory and have been shown to encode behavioral strategies. To examine the role of LPFC in overcoming working-memory limitations, we recorded the activity of LPFC neurons in animals trained to perform a serial self-ordered search task. This task measured the ability to prospectively plan the selection of unchosen spatial search targets while retrospectively tracking which targets were previously visited. We found that individual LPFC neurons encoded the spatial location of the current search target but also encoded the spatial location of targets up to several steps away in the search sequence. Neurons were more likely to encode prospective than retrospective targets. When subjects used a behavioral strategy of stereotyped target selection, mitigating the working-memory requirements of the task, not only did the number of selection errors decrease but there was a significant reduction in the strength of spatial encoding in LFPC. These results show that LPFC neurons have spatiotemporal mnemonic fields, in that their firing rates are modulated both by the spatial location of future selection behaviors and the temporal organization of that behavior. Furthermore, the strength of this tuning can be dynamically modulated by the demands of the task.

prefrontal | working memory | macaque

The capacity of working memory was empirically defined by Miller as 7 ± 2 items (1), although more recently this limit has been revised down to four items (2). These capacity limits seem hard to reconcile with our everyday experience, where we appear to have little problem temporarily remembering numbers of items at or beyond the empirical limit. This is partly due to the rigorous laboratory conditions under which capacity limits are measured, while in everyday life we use a repertoire of behavioral strategies to overcome these limits. For example, dealing a hand of cards to players in random order would necessarily involve a large working-memory load, requiring the dealer to keep track of how many cards each player has been dealt. By instead selecting a behavioral strategy, such as dealing the cards to players in a clockwise order, the dealer reduces the working-memory load to only a single item (last player dealt a card), enabling the task of dealing cards to be completed at a lower computational cost.

It remains unclear how these high-level strategies interact with the contents of working memory. A likely source for the neural basis of this interaction is the lateral prefrontal cortex (LPFC). Neurons in this area selectively encode task-specific information across intervening delay periods and distractors (3), consistent with maintaining information in working memory. Neurons in this region also encode high-level information about rules (4), categories (5), and strategies (6). The spatial self-ordered search task taxes both working memory and strategy use. This requires subjects to search through an array of targets collecting rewards, requiring monitoring of which targets were previously visited. Patients with prefrontal damage were impaired at the task (7) and experiments in monkeys showed that this was specifically due to damage of LPFC, as opposed to the neighboring frontal eye fields (8).

Neuroimaging studies have also revealed that LPFC shows greater activity as working-memory load increases (9, 10). This could simply reflect the increase in task difficulty as working-memory capacity is approached, since increasing task demands reliably increase activity in prefrontal cortex (11). However, when information is organized into a meaningful sequence, task difficulty decreases and behavioral performance increases, while blood oxygenation level-dependent activity in LPFC remains increased (12). Taken together these findings suggest that LPFC plays an important role in organizing information in working memory that is orthogonal to the working-memory demands of the task. In support of this, increasing the delay over which information must be remembered does not exacerbate the effects of LPFC damage on the self-ordered search task, whereas increasing the number of items that must be monitored does (13). To investigate how strategies and working memory interact at the single-neuron level in LPFC, we trained monkeys to perform a spatial self-ordered search task and recorded the activity of LPFC neurons.

Methods

We trained two rhesus monkeys to perform an oculomotor spatial self-ordered search task (Fig. 1*A*). Subjects were presented with a display of six targets and were required to select each target in turn. Subjects were allowed to select the targets in any order but only received a reward the first

Significance

Working memory is a capacity-limited system that is used by cognitive processes, such as planning, reasoning, and decision making, to temporarily store information for short periods of time. We often employ behavioral strategies to overcome the capacity limit, such as processing information in sequences, but how this is accomplished at the neural level is unknown. By recording the electrical activity of prefrontal neurons during working-memory tasks, we found that prefrontal neurons had spatiotemporal receptive fields, encoding both the spatial coordinates of behavioral targets and their organization within a sequence. Furthermore, the strength of this tuning could be dynamically modulated according to how much subjects relied on working memory or behavioral strategies.

Author contributions: F.-K.C. and J.D.W. designed research; F.-K.C. performed research; F.-K.C. and J.D.W. analyzed data; and F.-K.C. and J.D.W. wrote the paper.

The authors declare no conflict of interest.

This article is a PNAS Direct Submission.

[1]Present address: Department of Neuroscience and the Friedman Brain Institute, Icahn School of Medicine at Mount Sinai, New York, NY 10029.

[2]To whom correspondence should be addressed. Email: wallis@berkeley.edu.

This article contains supporting information online at www.pnas.org/lookup/suppl/doi:10.1073/pnas.1805044115/-/DCSupplemental.

Published online April 23, 2018.

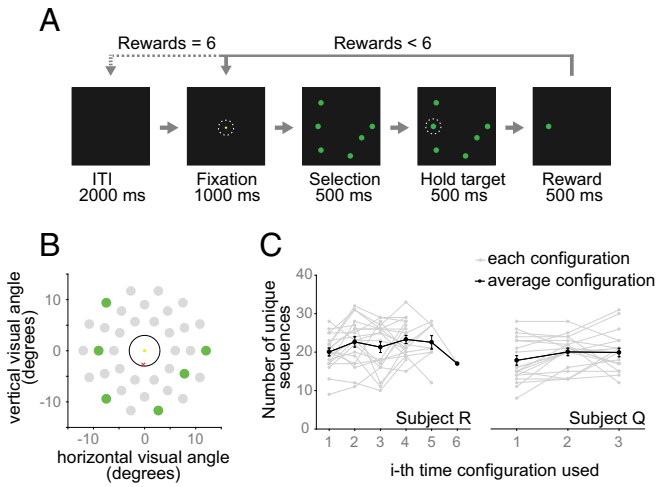

Fig. 1. (*A*) Spatial self-ordered search task. (*B*) Each configuration consisted of six targets (green filled circles), which were selected from 36 possible locations (gray filled circles). We ensured that targets were approximately balanced across the display by requiring that the centroid of the configuration (red cross) be located within ±3° of the fixation window (black circle). The intertarget distances were >6° to avoid overlap of the eye position detection window around the target. (*C*) Number of unique sequences of target selection per configuration.

time that a target was selected per trial. Revisiting a previously selected target resulted in a 500-ms time-out. Thus, subjects had to maintain in working memory which targets had already been selected. Once subjects received six rewards by selecting each target once, the current trial was terminated and an intertrial interval was initiated. The target–reward contingency reset at the beginning of a new trial.

Target configurations consisted of six identical targets, each 2° in diameter and located at one of 36 positions on the visual display (Fig. 1*B*). The subject had to saccade to each target in turn and fixate it for 500 ms. Fixation was defined as maintaining the eye position within ±3° of the center of the target. Any drift out of this window would reset the 500-ms fixation duration. After the successful fixation of a target, the outcome was determined according to whether or not the selected target had been previously selected on the current trial. In between each target selection, the targets disappeared and the fixation cue was presented. The subject had to fixate this cue for 1 s before the targets were presented again. To avoid excessive frustration, if the subject experienced more than 10 time-outs in a single trial then the trial was aborted. This happened on <1% of trials. To ensure that subjects realized that they had found all six possible rewards, the color of the targets changed from trial to trial in a green–white–blue sequence. The target configuration remained stable for a block of 40 trials, of which subjects completed six per session. The spatial configuration of targets used for each block was pseudorandomly chosen from a pool of 20 a priori-designed spatial configurations. The same configuration was presented repeatedly within a block but used only once per session.

We implanted both subjects with a head positioner for restraint and a titantium recording chamber over each hemisphere. Acutely, we recorded from bilateral LPFC using arrays of 16–32 tungsten microelectrodes (FHC Instruments). All procedures were in accord with the National Institute of Health guidelines and the recommendations of the University of California, Berkeley Animal Care and Use Committee. Further details are in *SI Appendix*.

Results

Task Performance. Subject R completed 15 sessions and subject Q completed 10 sessions, with each session comprising six blocks of 40 trials. One block of trials was excluded from subject Q as there were fewer than 20 complete trials in that block. To quantify task performance, we tabulated the number of revisited targets on each trial. Subjects performed the task at a high level (Fig. 2*A*); about 80% of trials were completed with two or fewer incorrect saccades.

To complete a trial, the subject needed to select each of the six targets once. We refer to these correct target selections as T_i, where i is the i^{th} selected target in the sequence $T_1 \ldots T_6$. We defined the success rate for each target selection T_i as the number of trials where the target was selected without any errors, divided by the total number of trials (Fig. 2*B*). We then used the average success rate across $T_1 \ldots T_6$ to calculate the expected success rate at each T_i, assuming that the overall probability of making a mistake is a linear function of the number of potentially incorrect saccades that are possible (*SI Appendix*). We then calculated whether the actual success rate significantly differed from the expected success rate using binomial tests. Both subjects made fewer correct saccades in selecting the fifth and sixth targets compared with the expected success rate (Fig. 2*B*; binomial test, $P < 0.001$). This suggests that the working-memory demands of the task increased as the number of selected targets increased and began to exceed the subjects' working-memory capacity by the fifth and sixth target selections.

We defined the saccadic reaction time (sRT) as the time from the onset of the target configuration to the beginning of the 500-ms hold target epoch (Fig. 2*C*). Incorrect saccades were excluded from the calculation of sRT. The overall median sRT was 210 and 221 ms from subjects R and Q, respectively. Further, we calculated sRT separately for each target selection and performed a linear regression using sRT as the dependent variable and the selected target's position in the selection sequence as a predictor. For both subjects, we found that sRT significantly increased as the number of selected targets increased [Fig. 2*B*; subject R: $F(1, 20{,}596) = 2{,}400$, $r^2 = 0.10$, $P < 1 \times 10^{-18}$; subject Q: $F(1, 12{,}491) = 81$, $r^2 = 0.006$, $P < 1 \times 10^{-18}$]. This could be an effect of exceeding working-memory capacity, or it might reflect the increased response selection requirements that arise from the increased number of targets that must be avoided.

Behavioral Strategies. We next analyzed the patterns of target selection to gain insight into the behavioral strategies that the subjects employed to solve the task. Each of the 20 configurations was pseudorandomly selected four to six times for subject R and three times for subject Q across the recording sessions. For each block of 40 trials using a specific spatial configuration, we

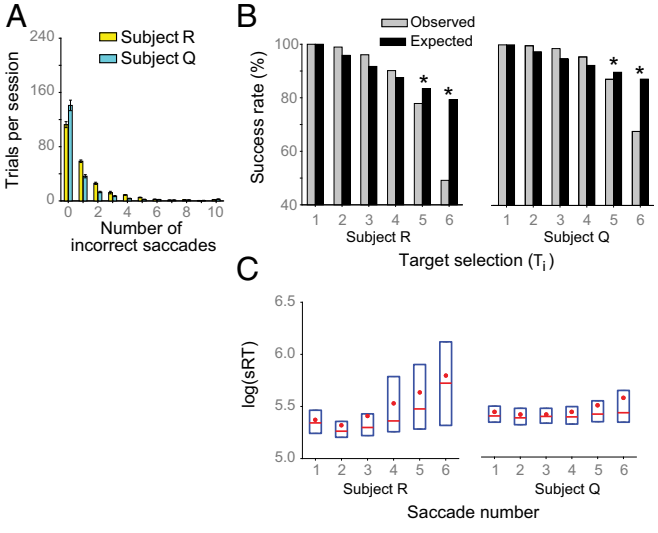

Fig. 2. Behavioral performance. (*A*) Distribution of the number of incorrect saccades per trial. (*B*) Observed and expected success rates plotted as a function of which target in the sequence was selected. The observed success rate was significantly lower than the expected error rate for the fifth and sixth selected targets in both subjects (binomial test, *$P < 0.001$). (*C*) Reaction times as a function of saccade. Box plots indicate the 25th, 50th, and 75th percentiles of the sRT distribution. Red dots indicate the mean sRT.

calculated the total number of unique sequences in which the subjects selected the six targets (Fig. 1*C*). Some configurations were associated with fewer numbers of unique sequences than others, suggesting that subjects approached these configurations using a more stereotyped strategy. Although some configurations were consistently associated with more stereotyped selection patterns than others, there was considerable variability, with the same configuration frequently exhibiting either more or less stereotyped selection patterns with subsequent presentations to the same subject. Furthermore, there was no relationship between the number of unique sequences and the number of times the configuration had been used in the task [Fig. 1*C*; subject R: $F(1, 88) = 1.47$, $r^2 = 0.016$, $P = 0.23$; subject Q: $F(1, 57) = 1.71$, $r^2 = 0.029$, $P = 0.20$]. In other words, there was no evidence that repeatedly experiencing the same configuration led to an increase in the use of stereotyped strategies.

To quantify the degree to which the subject's selection strategy was stereotyped, for each block of trials we calculated how often each target was selected by a specific target selection ($T_1 \ldots T_6$). We then used this information to construct the pseudocolor matrices shown in Fig. 3*A*. The *x* axis shows each of the six target selections. The *y* axis shows which of the six targets was selected, sorted according to the most common sequence in which the targets were selected. The color scale shows how frequently a given target selection was directed to a particular target. We used this data to calculate a stereotype index (SI), which quantified the extent to which the subject searched through the targets in the same sequence for all 40 trials within a block:

$$\mathrm{SI} = (a - b)/(a + b), \qquad [1]$$

where a is the sum of the entries on the main diagonal of the matrix and b is the off-diagonal sum of the matrix. Fig. 3*B* illustrates how the value of the SI index increased as the subjects' pattern of saccades became more stereotyped. Increased levels of stereotyped behavior significantly improved behavioral performance in both subjects, evident as a reduction in the number of incorrect saccades for both subjects [Fig. 3*C*; subject R: $F(1, 88) = 11$, $r^2 = 0.11$, $P < 0.005$; subject Q: $F(1,57) = 31$, $r^2 = 0.35$, $P < 1 \times 10^{-7}$].

Neurophysiological Analysis. We recorded from 1,077 LPFC neurons (R: 709; Q: 368), the majority of which were within the principal sulcus (*SI Appendix*, Fig. S1). For each neuron, we

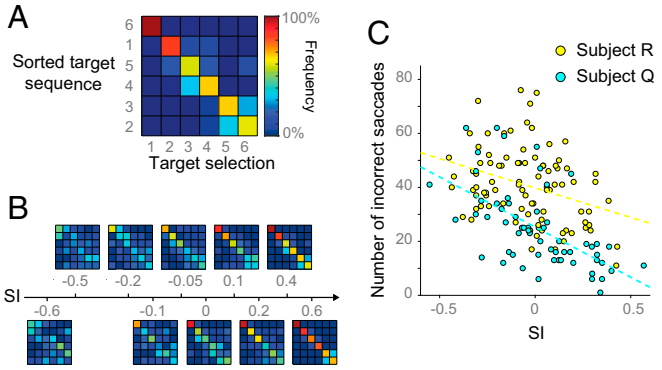

Fig. 3. (*A*) For each block of trials, we calculated how many times a particular target was selected for each target selection ($T_1 \ldots T_6$). We then plotted this data according to the most common sequence in which targets were selected. (*B*) Representative blocks, illustrating how the pseudocolor plots changed as a function of SI. Blocks above the line are from subject R, and blocks below the line are from subject Q. (*C*) Increased values of SI were correlated with better behavioral performance (fewer incorrect saccades).

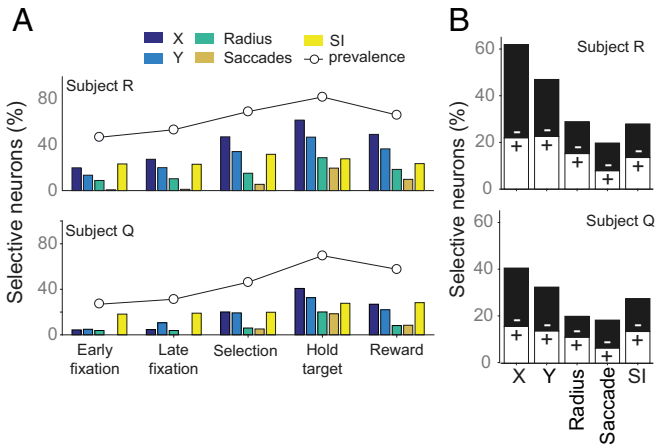

Fig. 4. (*A*) Percentage of selective neurons that encoded different predictors in each epoch. Black circles indicate the percentage of selective neurons defined as those that encoded at least one predictor during the epoch. (*B*) The proportion of beta coefficients with positive (+) or negative (–) values during the hold epoch.

calculated its mean firing rate (FR) during five trial epochs: early fixation, late fixation, selection, hold target, and reward. The early and late fixation epochs were defined as the first and second 500 ms of the fixation period. The selection epoch consisted of a 500-ms period, starting 150 ms before the onset of the targets until 350 ms after the onset. The hold target epoch comprised the 500-ms period of fixation required to select the target. The reward epoch was the first 500 ms of juice delivery following a correct saccade.

We used a multiple linear regression model to determine which aspects of the task each neuron encoded. For each neuron, we quantified the extent to which we could predict its mean FR in each epoch based on the following predictors: the *x* and *y* coordinates of the selected target, distance from the fixation cue to the target (radius), saccade number (one through six), and SI (Eq. **1**). We also included a nuisance parameter (trial number) that would capture gradual changes in the neuron's FR across the course of the session, for example, due to changes in the neuron's position relative to the recording electrode ("drift"). Significance was evaluated at $P < 0.01$. FRs and predictors were standardized to allow comparison of regression coefficients:

$$\begin{aligned}\mathrm{FR} = {} & b_1.\mathrm{X} + b_2.\mathrm{Y} + b_3.\mathrm{Radius} + b_4.\mathrm{Saccade\ number} \\ & + b_5.\mathrm{SI} + b_6.\mathrm{Trial\ number}.\end{aligned} \qquad [2]$$

We observed the maximum amount of encoding during the hold target epoch (Fig. 4*A*). Although most selective neurons encoded the spatial position of the target, the FRs of many neurons were also affected by SI. However, stereotypy did not consistently affect LPFC neuronal FRs; neurons were equally as likely to increase their FR as SI increased as they were to decrease their FR (Fig. 4*B*).

Encoding of Spatial Information. Since the majority of neurons were spatially selective in at least one epoch of the task, we examined how spatial selectivity evolved as the animal selected each target in turn. We examined how the neuron's FR, during a given epoch and for a given target selection, was predicted by the spatial location of each of the targets in the sequence. There were 12 predictors consisting of six pairs of *x* and *y* coordinates. We defined a neuron as significantly encoding a target's location if the full model was significant and the beta associated with either the *x* or *y* position of a target was significant at $P < 0.01$.

Fig. 5*A* illustrates how spatial selectivity for the targets changed as the sequence was completed. The most prevalent encoding, present in ∼35% of LPFC neurons in subject R and ∼20% in subject Q during the hold-target epoch, was the spatial location of the currently selected target, evident on the main diagonal of the pseudocolor matrices.

However, many neurons were also selective for targets that were not currently being selected (colors on the off-diagonals of the pseudocolor matrices), reflecting targets that had either been previously selected (lower left of the matrix) or would be selected in the future (upper right of the matrix). The maximally encoded target evolved over the course of trial events. During early fixation, the most recently selected target was encoded most strongly, particularly in subject R, and then spatial selectivity began to reflect the current target, peaking during the hold epoch. LPFC neurons encoded upcoming targets with stronger selectivity than those that had been previously selected (*SI Appendix*, Fig. S2). Beyond this trend, the responses of individual neurons were highly heterogeneous, reflecting different combinations of target locations encoded during different target selections, and most neurons encoded information about both past and future targets (*SI Appendix*, Fig. S3). There did not appear to be any overarching principle regarding the precise pattern of target locations that were encoded for each target selection, such as consistently encoding a specific step in the sequence, either in absolute terms or relative to the currently selected target.

To more precisely characterize the relationship between spatial and temporal information, for each neuron, we calculated the spatial tuning for each entry in the matrix that was significant during the hold epoch (*SI Appendix*). We focused on those entries containing significant spatial information (as determined by the regression) and calculated the angular difference between spatial tuning for pairs of targets with the same temporal relationship (e.g., past versus past), and pairs with different temporal relationships (e.g., past versus current). In both animals, comparisons between entries that were at the same temporal phase showed smaller angular differences in tuning than comparisons across temporal phases (Fig. 5*B*). We also made the same comparisons across neurons (i.e., comparing the same entries of the matrix but taken from different neurons that both showed significant spatial selectivity for those entries). In nearly all cases, within-neuron differences in spatial tuning were significantly different from between-neuron differences (*SI Appendix*, Fig. S4). Thus, even though the majority of LPFC neurons showed a mixture of spatial selectivity, encoding the location of past, present, and future targets, they exhibited relatively distinct spatial tuning for each temporal phase.

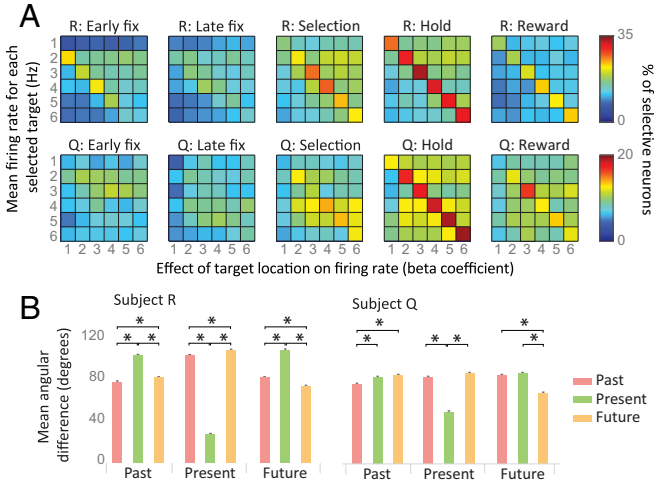

Fig. 5. (*A*) For each neuron, six regressions were performed using the mean FR of the neuron for each target selection, $T_1 \ldots T_6$, as the dependent variable (*y* axis). The color axis indicates the percentage of neurons that significantly encoded the spatial location of each of the targets in the sequence (*x* axis). Entries on the main diagonal represent neurons that encoded the currently selected target's spatial location. Entries below the main diagonal represent neurons that encoded the spatial location of previously selected targets. Entries above the main diagonal represent neurons that encoded the spatial location of upcoming targets. *Top* and *Bottom* are from subjects R and Q, respectively. (*B*) Mean angular difference in the spatial tuning of single neurons for pairs of significant matrix entries. The *x* axis and the color of the bar jointly specify the type of comparison. Brackets indicate significant differences (one-way ANOVA with Tukey–Kramer corrected post hoc tests, $*P < 0.01$). Spatial tuning for targets at the same temporal phase (e.g., past versus past) was more similar than tuning for targets at different temporal phases (e.g., past versus present).

Effects of Behavioral Strategy on Spatial Encoding. Many LPFC neurons showed a different degree of spatial encoding depending on whether the subject was performing the task using a stereotyped strategy. Fig. 6*A* shows two examples, one from each subject. In both cases, the neurons showed stronger encoding of spatial information when the animal was not using a stereotyped strategy. To quantify the prevalence of this encoding, we first identified spatially selective neurons as those which significantly encoded the current target's *x* and/or *y* coordinate based on the full regression model. We again focused on the hold-target epoch since this was when we observed the maximum amount of spatial selectivity. There were 740 spatially selective neurons (R: 529; Q: 211). For each neuron, we then applied a reduced regression model to each block of trials to quantify spatial tuning at the current target location:

$$FR = b_1.X + b_2.Y. \quad [3]$$

We then plotted the percentage of variance in the neuron's FR that could be explained by the spatial position of the targets as a function of SI, calculated from the r^2 of the reduced model. There was a significantly negative correlation between the r^2 and the magnitude of the SI in both subjects (Fig. 6*B*; subject R: $r = -0.047$, $P < 0.01$; subject Q: $r = -0.097$, $P < 0.001$). Spatial tuning also decreased for the same configuration display when the subject adopted a more stereotyped search strategy (*SI Appendix*, Fig. S5). Thus, when subjects performed the task using a more stereotyped strategy, LPFC neurons encoded less spatial information. However, although neurons showed less spatial tuning when subjects followed a more stereotyped search strategy, the direction of the tuning remained constant (*SI Appendix*, Fig. S6).

Discussion

We recorded the activity of LPFC neurons from two monkeys trained to perform a serial self-ordered search task (7, 14). There were three main findings of interest. First, individual LPFC neurons encoded the spatial location of the current search target but also encoded the location of other targets, even those several steps away in the search sequence. Second, LPFC neurons were more likely to encode upcoming targets than previously visited targets, although both were encoded well above chance. Finally, behavioral strategies that both monkeys spontaneously employed to help solve the task improved behavioral performance while simultaneously reducing the neuronal load required.

Role of Prefrontal Cortex in the Sequential Organization of Behavior. Prefrontal cortex is at the apex of the perception–action cycle, responsible for integrating sensory information and structuring behavior over long time scales (15). For example, damage to LPFC produces deficits in planning, both in laboratory tests (16) and everyday behavior (17). Neuroimaging and neuropsychology

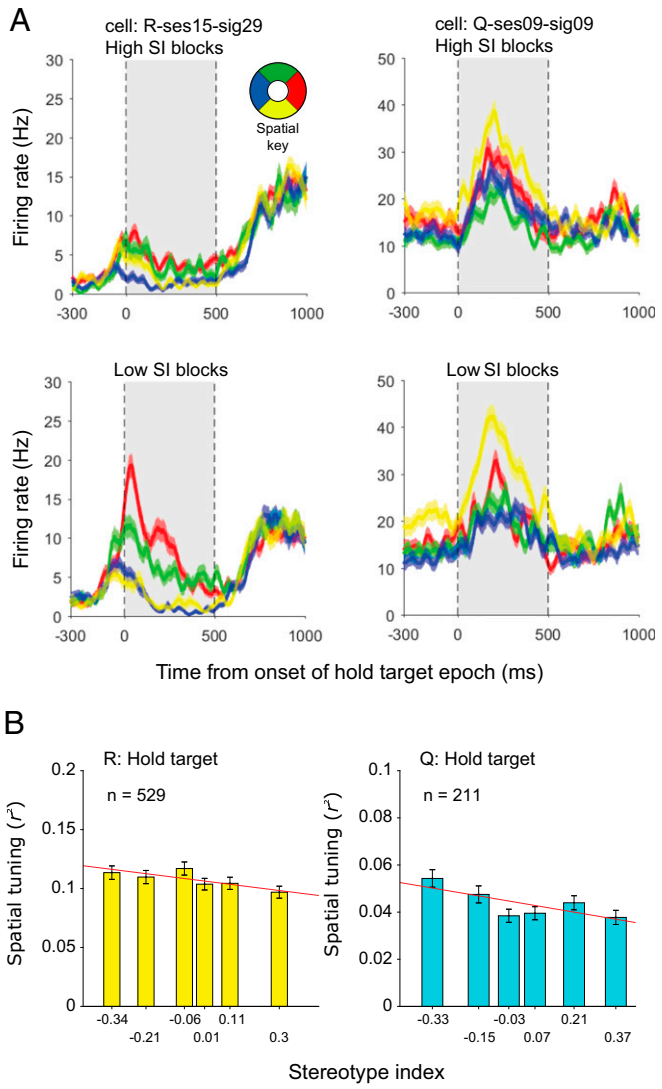

Fig. 6. (*A*) Single-neuron examples showing the effects of the stereotype strategy on spatial tuning. Spike density histograms are plotted from two neurons, one recorded in subject R (left two panels) and one recorded from subject Q (right two panels). The color of the plots refers to the position of the selected target on the screen, as shown in the key. Plots on the top are from the three blocks in the session with the higher SI, whereas the plots on the bottom are from the three blocks with the lower SI. Less spatial tuning was observed when the animal was searching through the targets using a more stereotyped strategy. (*B*) Spatial tuning, as measured by the r^2 from the reduced model, as a function of SI. Stronger spatial tuning occurred in blocks with less stereotyped behavior.

studies have shown that progressively more anterior regions of the frontal lobe are responsible for integrating behavior across progressively more complex and temporally extended task structures (18, 19). Neurophysiological recordings have shown that LPFC neurons encode information about specific actions, but this encoding often depends on how this action is embedded within a sequence of actions (20). At a more abstract level, population analyses have shown that the main information encoded by prefrontal neurons during the performance of a cognitive task is the sequence of events in the task (21). Prefrontal neurons have also been shown to encode high-level information, such as categories (5) and rules (4).

The above studies are consistent with a role for prefrontal cortex in structuring behavior at a high level. Our current results suggest a mechanism that helps to delineate a more precise role for prefrontal cortex in this process. LPFC neurons were strongly tuned for the spatial locations of targets, but this tuning was not restricted to just the current target, but rather included previous and upcoming targets, often several steps in the sequence from the current target. Furthermore, spatial tuning was more similar for targets at the same temporal phase of the sequence than for targets at different temporal phases. This was particularly the case for tuning related to the current location but was also apparent in the tuning for past and future targets. Upcoming actions tended to be represented more strongly than completed responses, which is consistent with previous studies that have also noted a bias toward prospective encoding in prefrontal neurons (22, 23).

Previous studies that have examined the contribution of LPFC neurons to working memory have concentrated on the ability of LPFC neurons to exhibit spatial tuning across intervening delays, so-called mnemonic receptive fields (22, 24–26). Our results extend this concept and suggest that a more complete description of prefrontal tuning is a spatiotemporal receptive field that encompasses both the spatial coordinates of the target behavior as well its temporal order within the behavioral structure. Our results are consistent with recent models of prefrontal cortex that have emphasized the high-dimensional nature of prefrontal encoding schemes, particularly the mixed selectivity models (27, 28), since the spatial selectivity of an individual prefrontal neuron is not fixed but rather depends on the temporal phase of the task.

The spatial self-ordered search task was developed by Petrides and Milner because patients with prefrontal damage performed remarkably well on short-term memory tests, such as digit span and story recall (7, 29). This contrasted with the severe deficits that these patients exhibited on tasks that required planning (16, 17) or flexible control of behavior (30). Indeed, recent studies have shown that prefrontal damage does not impair classic tasks of spatial working memory, such as the memory-guided saccade task, so long as the frontal eye fields are preserved (31). Petrides has argued that the critical feature of the self-ordered search task that makes it sensitive to prefrontal damage is the requirement to attend to all stimuli within the set and monitor successive choices, in other words, tracking which stimuli have been selected and which have not been selected. The spatiotemporal receptive fields that we observed in LPFC neurons contain precisely the information that would be needed for this process, encoding both the current target of behavior as well as which stimuli have been and will be selected.

Role of PFC in Cognitive Control. When subjects searched through the targets in a more stereotyped way, their behavioral performance improved, despite a drop in the amount of spatial information that was encoded in LPFC. Our previous studies looked at the effects of reward on LPFC spatial tuning (32). If a reward-predictive cue was presented before a memorandum, then LPFC neurons showed stronger spatial tuning and behavioral performance improved. However, presenting the reward-predictive cue after the memorandum was distracting. Under these conditions, LPFC neurons showed weaker tuning and behavioral performance declined. Thus, behavioral performance correlated with the strength of LPFC spatial tuning. Taken together with our current results, this shows that the prefrontal representation of space is highly dynamic and the strength of tuning can change in response to the cognitive demands of the task. However, our current results contrast with this previous study, in that loss of spatial tuning was correlated with an improvement in behavioral performance.

One possibility is that using a stereotyped strategy to search through the targets recruits other brain regions more involved in sequence learning, thereby reducing the need for prefrontal

working-memory mechanisms (33). Neuroimaging studies have shown a shift from a prefrontal-cerebellar network to a premotor-striatal network as a motor sequence becomes more stereotyped and performance more automatic (34, 35). Neural recordings in the supplementary motor area have revealed neurons that encode specific sequences of movements, while inactivation of this area impairs the performance of a motor sequence, but not the execution of individual movements (36). One advantage of automation with skill development is that it frees up attentional resources for other tasks, which would be consistent with a drop in prefrontal tuning, if LPFC is indeed responsible for the allocation of these resources.

In sum, our data show that prefrontal coding of information relevant to working memory can be dynamically modulated according to task demands. Consequently, the implementation of behavioral strategies to reduce performance demands can change the information content of prefrontal neurons. This has implications for computational accounts of working memory, which are described as bump attractors, whereby persistent population codes are maintained through a combination of local recurrent excitation and broader feedback inhibition (37, 38). The capacity limits of working memory are thought to arise because drift in the attractors can cause adjacent bumps to merge or fade, which becomes more likely as the number of attractor states increases (39, 40). A read-out problem could arise if the size of the bumps can be modulated by other factors, such as task demands. If a downstream brain area were receiving information solely from LPFC, there would be ambiguity as to whether noise in the representation arose from the capacity limits of the prefrontal representation or whether it reflected a handing off of the storage functions to other brain areas. In reality, this may be less of a problem, since most areas are receiving information from many different brain areas, and could, in principle, "listen" to the area with the most robust response. Future research could test this hypothesis, by comparing the strength of the spatial representation in downstream areas, such as the striatum and premotor cortex, with that observed in LPFC during performance of the self-ordered search task.

ACKNOWLEDGMENTS. We thank Eric Knudsen for comments on the manuscript. This work was funded by National Institute of Mental Health Grant R01 MH097990 (to J.D.W.) and by Taiwan Top University Strategic Alliance Graduate Fellowship USA-UCB-100-S01 (to F.-K.C.).

1. Miller GA (1956) The magical number seven plus or minus two: Some limits on our capacity for processing information. *Psychol Rev* 63:81–97.
2. Cowan N (2001) The magical number 4 in short-term memory: A reconsideration of mental storage capacity. *Behav Brain Sci* 24:87–114, discussion 114–185.
3. Miller EK, Erickson CA, Desimone R (1996) Neural mechanisms of visual working memory in prefrontal cortex of the macaque. *J Neurosci* 16:5154–5167.
4. Wallis JD, Anderson KC, Miller EK (2001) Single neurons in prefrontal cortex encode abstract rules. *Nature* 411:953–956.
5. Freedman DJ, Riesenhuber M, Poggio T, Miller EK (2001) Categorical representation of visual stimuli in the primate prefrontal cortex. *Science* 291:312–316.
6. White IM, Wise SP (1999) Rule-dependent neuronal activity in the prefrontal cortex. *Exp Brain Res* 126:315–335.
7. Petrides M, Milner B (1982) Deficits on subject-ordered tasks after frontal- and temporal-lobe lesions in man. *Neuropsychologia* 20:249–262.
8. Petrides M (1995) Impairments on nonspatial self-ordered and externally ordered working memory tasks after lesions of the mid-dorsal part of the lateral frontal cortex in the monkey. *J Neurosci* 15:359–375.
9. Emrich SM, Riggall AC, Larocque JJ, Postle BR (2013) Distributed patterns of activity in sensory cortex reflect the precision of multiple items maintained in visual short-term memory. *J Neurosci* 33:6516–6523.
10. Rypma B, Prabhakaran V, Desmond JE, Glover GH, Gabrieli JD (1999) Load-dependent roles of frontal brain regions in the maintenance of working memory. *Neuroimage* 9: 216–226.
11. Crittenden BM, Duncan J (2012) Task difficulty manipulation reveals multiple demand activity but no frontal lobe hierarchy. *Cereb Cortex* 24:532–540.
12. Bor D, Duncan J, Wiseman RJ, Owen AM (2003) Encoding strategies dissociate prefrontal activity from working memory demand. *Neuron* 37:361–367.
13. Petrides M (2000) Dissociable roles of mid-dorsolateral prefrontal and anterior inferotemporal cortex in visual working memory. *J Neurosci* 20:7496–7503.
14. Owen AM, Downes JJ, Sahakian BJ, Polkey CE, Robbins TW (1990) Planning and spatial working memory following frontal lobe lesions in man. *Neuropsychologia* 28: 1021–1034.
15. Fuster JM (2001) The prefrontal cortex–An update: Time is of the essence. *Neuron* 30: 319–333.
16. Shallice T (1982) Specific impairments of planning. *Philos Trans R Soc Lond B Biol Sci* 298:199–209.
17. Shallice T, Burgess PW (1991) Deficits in strategy application following frontal lobe damage in man. *Brain* 114:727–741.
18. Badre D, D'Esposito M (2007) Functional magnetic resonance imaging evidence for a hierarchical organization of the prefrontal cortex. *J Cogn Neurosci* 19:2082–2099.
19. Badre D, Hoffman J, Cooney JW, D'Esposito M (2009) Hierarchical cognitive control deficits following damage to the human frontal lobe. *Nat Neurosci* 12:515–522.
20. Averbeck BB, Sohn JW, Lee D (2006) Activity in prefrontal cortex during dynamic selection of action sequences. *Nat Neurosci* 9:276–282.
21. Sigala N, Kusunoki M, Nimmo-Smith I, Gaffan D, Duncan J (2008) Hierarchical coding for sequential task events in the monkey prefrontal cortex. *Proc Natl Acad Sci USA* 105:11969–11974.
22. Funahashi S, Bruce CJ, Goldman-Rakic PS (1989) Mnemonic coding of visual space in the monkey's dorsolateral prefrontal cortex. *J Neurophysiol* 61:331–349.
23. Rainer G, Rao SC, Miller EK (1999) Prospective coding for objects in primate prefrontal cortex. *J Neurosci* 19:5493–5505.
24. Fuster JM, Alexander GE (1971) Neuron activity related to short-term memory. *Science* 173:652–654.
25. Kubota K, Niki H (1971) Prefrontal cortical unit activity and delayed alternation performance in monkeys. *J Neurophysiol* 34:337–347.
26. Constantinidis C, Franowicz MN, Goldman-Rakic PS (2001) The sensory nature of mnemonic representation in the primate prefrontal cortex. *Nat Neurosci* 4:311–316.
27. Fusi S, Miller EK, Rigotti M (2016) Why neurons mix: High dimensionality for higher cognition. *Curr Opin Neurobiol* 37:66–74.
28. Rigotti M, et al. (2013) The importance of mixed selectivity in complex cognitive tasks. *Nature* 497:585–590.
29. Petrides M (2000) Impairments in working memory after frontal cortical excisions. *Adv Neurol* 84:111–118.
30. Milner B (1963) Effects of different brain lesions on card sorting. *Arch Neurol* 9: 100–110.
31. Mackey WE, Devinsky O, Doyle WK, Meager MR, Curtis CE (2016) Human dorsolateral prefrontal cortex is not necessary for spatial working memory. *J Neurosci* 36: 2847–2856.
32. Kennerley SW, Wallis JD (2009) Reward-dependent modulation of working memory in lateral prefrontal cortex. *J Neurosci* 29:3259–3270.
33. Desrochers TM, Burk DC, Badre D, Sheinberg DL (2016) The monitoring and control of task sequences in human and non-human primates. *Front Syst Neurosci* 9:185.
34. Doyon J, et al. (2002) Experience-dependent changes in cerebellar contributions to motor sequence learning. *Proc Natl Acad Sci USA* 99:1017–1022.
35. Floyer-Lea A, Matthews PM (2004) Changing brain networks for visuomotor control with increased movement automaticity. *J Neurophysiol* 92:2405–2412.
36. Shima K, Tanji J (1998) Role for cingulate motor area cells in voluntary movement selection based on reward. *Science* 282:1335–1338.
37. Compte A, Brunel N, Goldman-Rakic PS, Wang XJ (2000) Synaptic mechanisms and network dynamics underlying spatial working memory in a cortical network model. *Cereb Cortex* 10:910–923.
38. Wimmer K, Nykamp DQ, Constantinidis C, Compte A (2014) Bump attractor dynamics in prefrontal cortex explains behavioral precision in spatial working memory. *Nat Neurosci* 17:431–439.
39. Burak Y, Fiete IR (2012) Fundamental limits on persistent activity in networks of noisy neurons. *Proc Natl Acad Sci USA* 109:17645–17650.
40. Wei Z, Wang XJ, Wang DH (2012) From distributed resources to limited slots in multiple-item working memory: A spiking network model with normalization. *J Neurosci* 32:11228–11240.